Resistive switching in metal–ferroelectric–metal junctions

J. Rodríguez Contreras, H. Kohlstedt,[a] U. Poppe, and R. Waser
Institut für Festkörperforschung IFF, Forschungszentrum Jülich, 52425 Jülich, Germany

C. Buchal
Institut für Schichten und Grenzflächen ISG, Forschungszentrum Jülich, 52425 Jülich, Germany

N. A. Pertsev
A. F. Ioffe Physico-Technical Institute, Russian Academy of Sciences, 194021 St. Petersburg, Russia

(Received 30 May 2003; accepted 29 September 2003)

The aim of this work is to investigate the electron transport through metal–ferroelectric–metal (MFM) junctions with ultrathin barriers in order to determine its dependence on the polarization state of the barrier. To that end, heteroepitaxial Pt/Pb($Zr_{0.52}Ti_{0.48}$)O_3/$SrRuO_3$ junctions have been fabricated on lattice-matched $SrTiO_3$ substrates. The current–voltage ($I-V$) characteristics of the MFM junctions involving a few-nanometer-thick Pb($Zr_{0.52}Ti_{0.48}$)O_3 barriers have been recorded at temperatures between 4.2 K and 300 K. Typical $I-V$ curves exhibit reproducible switching events at well-defined electric fields. The mechanism of charge transport through ultrathin barriers and the origin of the observed resistive switching effect are discussed. © *2003 American Institute of Physics.* [DOI: 10.1063/1.1627944]

During the past few years, there has been considerable progress in understanding the size effects in ultrathin ferroelectric films. Nowadays, the theoretical work predicts[1–3] and experimental studies demonstrate[4,5] the presence of ferroelectricity in films as thin as a few unit cells.

The purpose of this work is to investigate the fundamental relation between the electron transport through metal–ferroelectric–metal (MFM) devices with ultrathin barriers and the polarization state of a barrier. If the thickness of a ferroelectric layer is small enough, the dominant transport mechanism may be even the direct quantum mechanical electron tunneling across the whole barrier. The sketch in Fig. 1 shows a simplified band diagram of a MFM heterostructure. The ferroelectric barrier is represented by a unit cell of Pb($Zr_{0.52}Ti_{0.48}$)O_3, which has two ground polarization states denoted by (1) and (2). We have chosen Pb($Zr_{0.52}Ti_{0.48}$)O_3 as an appropriate ferroelectric material in view of its high remanent polarization $P_r \approx 50\ \mu C/cm^2$, and because Pb($Zr_{1-x}Ti_x$)$O_3$ solid solutions exhibit a high piezoelectric response at the morphotropic phase boundary ($x \approx 0.5$). For the realization of an epitaxial MFM junction, we used $SrRuO_3$ as an electrode material since it shows extremely low surface roughness.[6] Single crystals of $SrTiO_3$ represent an appropriate substrate, which induces compressive in-plane strains in Pb($Zr_{0.52}Ti_{0.48}$)O_3 films and thus stabilizes the out-of-plane polarization state.[2] All oxide layers have been grown epitaxially, and a sharp Pb($Zr_{0.52}Ti_{0.48}$)O_3/$SrRuO_3$ interface was demonstrated in high-resolution transmission electron microscopy.[7] More details about the film deposition and structural investigations by x-ray diffraction, Rutherford backscattering spectrometry, and atomic force microscopy have been published elsewhere.[8]

In order to study the charge transport through a ferroelectric layer, MFM junctions involving Pb($Zr_{0.52}Ti_{0.48}$)O_3 barriers, with thicknesses ranging from 4 nm to 6 nm and with tunnel-junction areas between 4 μm^2 and 200 μm^2, were fabricated by means of photolithography and ion beam etching. The fabrication procedure is described in Ref. 8; it is similar to that of manganite tunnel junctions.[9,10] A top view of the experimental setup and a cross-sectional view of a MFM junction based on a Pt/Pb($Zr_{0.52}Ti_{0.48}$)O_3/$SrRuO_3$ heterostructure are shown schematically in Figs. 2(a) and 2(b), respectively. The current–voltage ($I-V$) measurements were

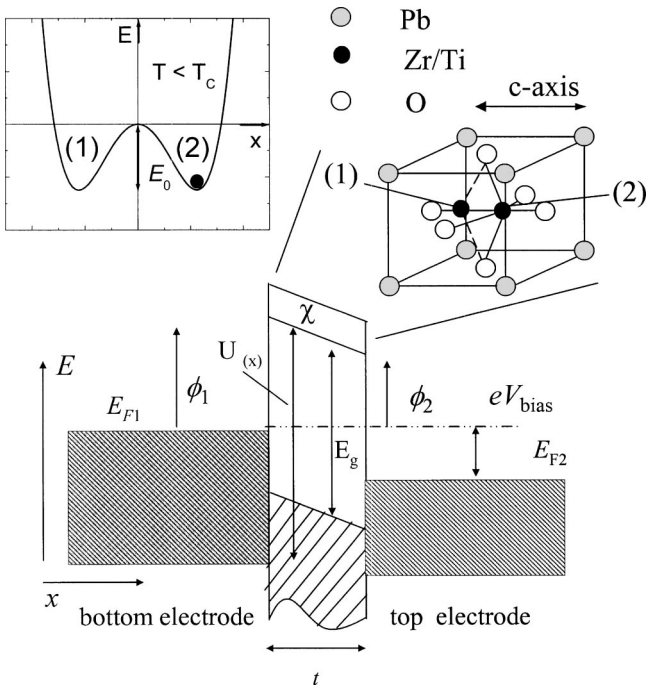

FIG. 1. Simplified band diagram of a MFM junction. E_F is the Fermi energy, χ is the electron affinity of the insulator, t is the barrier thickness, and ϕ_1, ϕ_2 are the barrier heights at the bottom and top electrode, respectively. The inserted sketch shows the structure of a unit cell of Pb($Zr_{0.52}Ti_{0.48}$)O_3 representing the ferroelectric barrier. Possible equilibrium positions of the Zr (or Ti) atom are labeled with numbers (1) and (2). The plot illustrates how the energy of a ferroelectric varies with the displacement of Zr (or Ti) atoms relative to the unit-cell center.

[a]Author to whom correspondence should be addressed; electronic mail: h.h.kohlstedt@fz-juelich.de

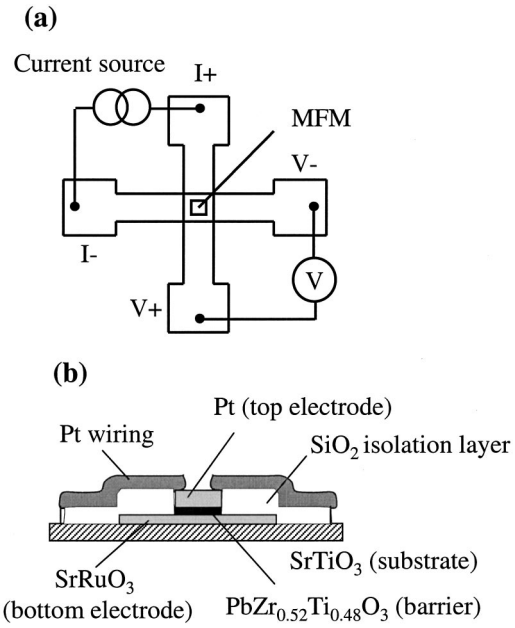

FIG. 2. Schematic illustration of a top view of the experimental setup (a) and a cross-sectional view of a MFM junction (b).

performed in a four-point arrangement to eliminate lead resistances. A battery-powered current source was used in these measurements, though the abscissa in the graphs, in Fig. 3, discussed below gives the voltage.

Figure 3(a) shows a typical $I-V$ characteristic of a 6-nm-thick $Pb(Zr_{0.52}Ti_{0.48})O_3$ film. The time for one complete cycle was 10 min. Numbers from 1 to 8 and arrows indicate the direction of scan. The $I-V$ curve displays clear switching events at $V^{-}_{\text{Switching}}=-0.54$ V and $V^{+}_{\text{Switching}}=0.86$ V and a crossover at the origin. The switching is highly reproducible and bistable. An asymmetric shape of the $I-V$ characteristic in these junctions (area $\approx 200\ \mu m^2$) most likely arises from different work functions at the $Pt/Pb(Zr_{0.52}Ti_{0.48})O_3$ and $Pb(Zr_{0.52}Ti_{0.48})O_3/SrRuO_3$ interfaces. The high- and low-resistance states are characterized by the resistances of 4.3 kΩ and 1.1 kΩ at the origin so that the resistance ratio is close to 4. When the dynamic conductance dI/dV is plotted versus voltage V [see Fig. 3(b)], the plot demonstrates a parabolic dependence. The asymmetry of

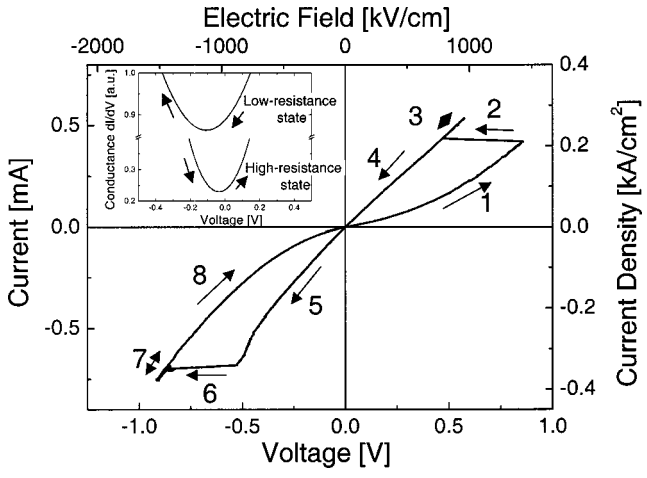

FIG. 3. Typical and highly reproducible $I-V$ characteristic of a 6-nm-thick $PbZr_{0.52}Ti_{0.48}O_3$ thin film. Inset: Dynamic conductance dI/dV plotted vs voltage for the low- and high-resistance states.

$I-V$ curves manifests itself in a shift of the conductance minimum relative to zero voltage.

What is the reason for the resistive switching? Similar switching processes in thin films have been reported for a variety of material systems.[11–13] For our purposes, the most relevant are the results of Watanabe,[14] and the IBM research group, Switzerland,[15–17] obtained in the last few years for complex perovskite devices. The IBM research group studied (35–300)-nm-thick $SrZrO_3$ films doped with 0.2% Cr,[15–16] as well as Cr-doped $SrTiO_3$ single crystals with a thickness of 10 μm.[17] A striking property observed for both thin films and single crystals is the multilevel switching in their $I-V$ curves. Different low-resistance states can be addressed by varying the length and amplitude of the applied voltage pulse. Their $I-V$ characteristics show some interesting similarities with our $I-V$ curves. Nevertheless, we believe that the transport mechanism and the origin of switching effects are different. Our assumption is based on the following distinctions. First, the thickness of our films is smaller by at least one order of magnitude, and the resistive switching of the type shown in Fig. 3(a) for a 6-nm-thick $Pb(Zr_{0.52}Ti_{0.48})O_3$ film was not observed for 12-nm-thick barriers. Second, we do not reveal multilevel resistance states in our MFM junctions. And finally, the temperature dependence of the resistance reported in Ref. 17 by the IBM group differs qualitatively from the one displayed by our films, where the resistance decreases with increasing temperature.

To check whether or not the reported switching effect may reflect the polarization reversal inside the ferroelectric barrier, we compared the critical electric field $E_{\text{Switching}}$, which characterizes the resistive switching observed in (4–6)-nm-thick $Pb(Zr_{0.52}Ti_{0.48})O_3$ films, with the coercive field E_c extracted from the polarization hysteresis loops of thicker $Pb(Zr_{0.52}Ti_{0.48})O_3$ films. We determined $E_{\text{Switching}}$ from the mean switching voltage $V_{\text{Switching}}=1/2(|V^{-}_{\text{Switching}}|+V^{+}_{\text{Switching}})$ to allow for the asymmetry of $I-V$ curves. The coercive voltage V_c is approximately the same for the thinnest capacitors, irrespective of their thickness, and so is the critical voltage of the MFM junctions [see Fig. 4(a)]. At the same time, both the coercive field E_c and the critical field $E_{\text{Switching}}$ increase rapidly with decreasing thickness in the nanometer range [see Fig. 4(b)]. The extrapolation of the coercive voltage and field to the thicknesses of our MFM junctions does not fit the data for the resistive switching. However, owing to the well-known frequency dependence of the coercive field[18] and a much lower frequency of the $I-V$ measurements, the critical voltage and field of the resistive switching are indeed expected to be lower than the extrapolated coercive voltage and field.

Though it might be just a coincidence, a good agreement between the thickness dependence of the coercive field E_c and that of the critical field $E_{\text{Switching}}$ strongly indicates the same origin of both discussed phenomena. Thus, the resistive switching in ultrathin ferroelectric films is probably due to the polarization reversal in the barrier. A proof of the ferroelectric origin of the resistive switching could be possible if a ferroelectric material with a low ferroelectric to paraelectric phase transition temperature, e.g., $T_c<100$ K is used. For such a material, the resistive switching should disappear in the paraelectric state. Due to the fact that the switching volt-

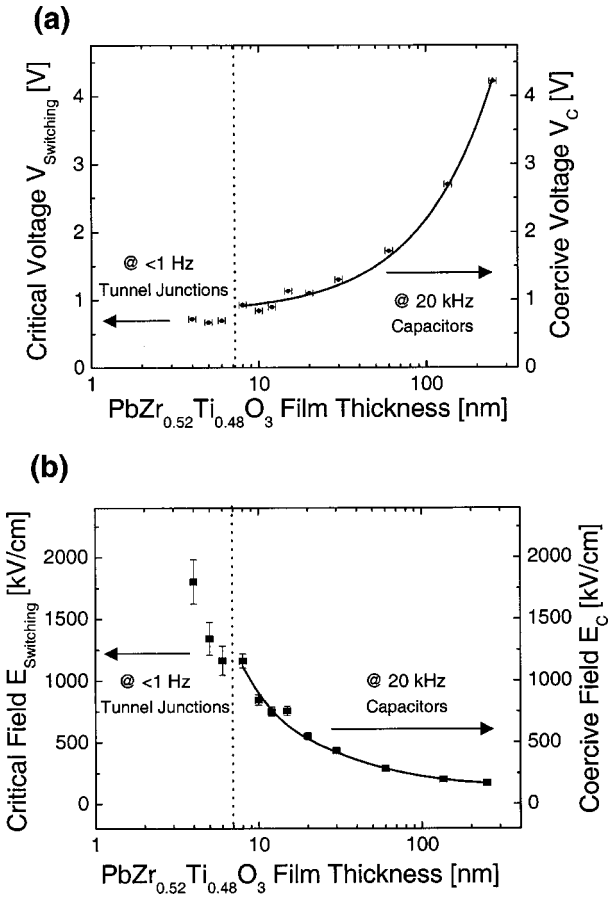

FIG. 4. Thickness dependence of the coercive and resistive switching voltages (a) and the coercive and resistive switching fields (b) measured for thick-film capacitors ($t \geqslant 8$ nm) and ultrathin MFM junctions ($t \leqslant 6$ nm), respectively.

age is a function of temperature, switching fields far below any breakdown are achievable and the effect could be observed at low-field stress. In addition, the low temperature will reduce the contribution of ionic transport mechanisms.

We will now discuss the mechanism of charge transport through our 6-nm-thick $Pb(Zr_{0.52}Ti_{0.48})O_3$ films. In order to check on the presence of direct electron tunneling between the electrodes, the $I-V$ curves of Pt/6 nm$-Pb(Zr_{0.52}Ti_{0.48})O_3/SrRuO_3$ junctions have been fitted by the Brinkman equation.[19] This procedure makes it possible to extract the apparent barrier thickness t and the barrier heights ϕ_1 and ϕ_2 (see Fig. 1). At 300 K, the barrier heights were determined to be $\phi_{1,\mathrm{low}} \approx 0.5$ eV, $\phi_{2,\mathrm{low}} \approx 0.3$ eV for the low-resistance state, and $\phi_{1,\mathrm{high}} \approx 0.3$ eV, $\phi_{2,\mathrm{high}} \approx 0.6$ eV for the high-resistance state. The barrier thickness was found to be $t_{\mathrm{low}} \approx 2.2$ nm and $t_{\mathrm{high}} \approx 2.3$ nm for the low- and high-resistance states, respectively. For lower temperatures, the barrier thickness found via the Brinkman equation increases. At 4.2 K, the Brinkman fit yields a barrier thickness of 4.3 nm and 5.2 nm for the low- and high-resistance states in reasonable agreement with the measured film thickness of 6 nm. However, the barrier heights (~ 0.1 eV for both states) are about five times smaller than expected.[20]

The Brinkman equation takes into account only the direct tunneling. In this case, electrons tunnel elastically across the whole barrier without any interaction with the material inside it. In real junctions, however, additional current paths through the barrier may exist thus leading to unrealistic parameters extracted from the Brinkman fit. At temperatures well above 0 K, in parallel, thermally assisted transport mechanisms have to be taken into account. Besides, the presence of localized states in the barrier influences the conductance of films having thicknesses much larger than the localization length. Strong contributions of phonon-assisted inelastic tunneling transport processes are believed to be present.

In summary, we have fabricated MFM junctions with a $Pb(Zr_{0.52}Ti_{0.48})O_3$ film thickness ranging from 4 to 6 nm. Typical $I-V$ characteristics exhibit two well-defined stable and reproducible resistance states. The critical fields of resistive switching are in line with the coercive field of capacitors containing slightly thicker (8 nm) ferroelectric films. This result suggests the polarization reversal in the ferroelectric barrier to be the origin of the observed resistive switching. Phonon-assisted inelastic tunneling processes are likely to be the dominant transport mechanism through 6-nm-thick $Pb(Zr_{0.52}Ti_{0.48})O_3$ films in the temperature range from 4.2 K to 300 K. Although a ferroelectric origin of the resistive switching events does not contradict the measured $I-V$ curves, more work is necessary to determine the influence of ferroelectricity on the quantum mechanical tunneling through ultrathin films.

The work was partly supported by the HGF-Strategiefonds "Piccolo" and the Volkswagen-Stiftung Project "Nanosized ferroelectric hybrids" under Contract No. I/77 737.

[1] J. Junquera and P. Ghosez, Nature (London) **422**, 506 (2003).
[2] A. G. Zembilgotov, N. A. Pertsev, H. Kohlstedt, and R. Waser, J. Appl. Phys. **91**, 2247 (2002).
[3] H. Kohlstedt, N. A. Pertsev, and R. Waser, Mater. Res. Soc. Symp. Proc. **688**, 161 (2002).
[4] T. Tybell, C. H. Ahn, and J.-M. Triscone, Appl. Phys. Lett. **75**, 856 (1999).
[5] S. K. Streiffer, J. A. Eastman, D. D. Fong, C. Thompson, A. Munkholm, M. V. Ramana Murty, O. Auciello, G. R. Bai, and G. B. Stephenson, Phys. Rev. Lett. **89**, 067601 (2002).
[6] C. B. Eom, R. J. Cava, R. M. Fleming, J. M. Philips, R. B. van Dover, J. H. Marshall, J. W. P. Hsu, J. J. Krajewski, and W. F. Speck, Jr., Science **258**, 1766 (1992).
[7] C. L. Jia, J. Rodríguez Contreras, U. Poppe, H. Kohlstedt, R. Waser, and K. Urban, J. Appl. Phys. **92**, 101 (2002).
[8] J. Rodríguez Contreras, J. Schubert, U. Poppe, O. Trithaveesak, K. Szot, C. Buchal, H. Kohlstedt, and R. Waser, Mater. Res. Soc. Symp. Proc. **688**, C8.10 (2002).
[9] J. Z. Sun, L. Krusin-Elbaum, P. R. Duncombe, A. Gupta, and R. B. Laibowitz, Appl. Phys. Lett. **70**, 1769 (1997).
[10] Y. Lu, X. W. Li, G. Q. Gong, G. Xiao, A. Gupta, P. Lecoeur, J. Z. Sun, Y. Y. Wang, and V. P. David, Phys. Rev. B **54**, 8357 (1996).
[11] S. R. Ovshinsky, Phys. Rev. Lett. **36**, 1469 (1968).
[12] K. L. Chopra, J. Appl. Phys. **36**, 184 (1965).
[13] J. F. Gibbons and W. E. Beadle, Solid-State Electron. **7**, 785 (1964).
[14] Y. Watanabe, Phys. Rev. B **59**, 11257 (1999).
[15] A. Beck, J. G. Bednorz, C. Gerber, C. Rossel, and D. Widmer, Appl. Phys. Lett. **77**, 139 (2000).
[16] C. Rossel, G. I. Meijer, D. Brémaud, and D. Widmer, J. Appl. Phys. **90**, 2892 (2001).
[17] Y. Watanabe, J. G. Bednorz, A. Bietsch, C. Gerber, D. Widmer, A. Beck, and S. J. Wind, Appl. Phys. Lett. **78**, 3738 (2001).
[18] Y. Ishibashi and H. Orihara, Integr. Ferroelectr. **9**, 57 (1995).
[19] W. F. Brinkman, R. C. Dynes, and J. M. Rowell, J. Appl. Phys. **41**, 1915 (1970).
[20] C. Sudhama, A. C. Campbell, P. D. Maniar, R. E. Jones, R. Moazzami, C. J. Mogab, and J. C. Lee, J. Appl. Phys. **75**, 1014 (1994).